Surface-Enhanced Hyper-Raman Scattering (SEHRS) on Ag Film over Nanosphere (FON) Electrodes: Surface Symmetry of Centrosymmetric Adsorbates†

John C. Hulteen, Matthew A. Young, and Richard P. Van Duyne*

Department of Chemistry, Northwestern University, Evanston, Illinois 60208

Received May 2, 2006. In Final Form: July 28, 2006

Electrochemical surface-enhanced hyper-Raman scattering (SEHRS) and surface-enhanced Raman scattering (SERS) of centrosymmetric molecules on Ag film over nanosphere (AgFON) electrodes are presented. The SEHR spectra of *trans*-1,2-bis(4-pyridyl)ethylene (BPE) at different potentials (vs Ag/AgCl) are presented for the first time, and a reversible potential tuning of the SEHR spectra of BPE is demonstrated. The SEHRS and SERS techniques were used to determine to what extent either site symmetry reduction or field gradient effects dictate the origin of the observed vibrational spectra. It is found that the SEHR and SER spectra for the molecules studied were distinctly different at all frequency regions at a fixed voltage, suggesting that centrosymmetry is largely retained upon adsorption to the AgFON surface and that field gradient effects are negligible. This work also shows that the SEHR spectra clearly depend on potential, whereas the SER spectra are essentially independent of potenial. It is determined that the combination of changes in ΔG_{ads} and the presence of coadsorbed counterions are responsible for altering the local symmetry of the adsorbate and only SEHRS has the sensitivity to detect these changes in the surface environment. Thus, SEHRS is a uniquely useful spectroscopic tool that is much more sensitive to the local adsorption environment than is SERS.

Introduction

Hyper-Raman scattering (HRS) is a nonlinear effect that is characterized by a scattering signal that is Raman shifted relative to the second harmonic of the excitation frequency (i.e., $\omega = 2\omega_0 - \Delta\omega$, where $\Delta\omega$ is the vibrational frequency). Because three photons are involved in this process, the selection rules for HRS are very different than for normal Raman spectroscopy (NRS), in which two photons are involved. Selection rules are an essential component in the analysis of surface vibrational spectra of adsorbed molecules. The vibrational frequency, intensity, and line shape characteristics can be used to determine molecular symmetry, orientation, and bond identities. When molecules are adsorbed on a metal surface, the band intensities can be modified as a result of surface interactions with the electromagnetic fields, known as "surface selection rules." For example, in surface infrared spectroscopy on metals,[1−5] only adsorbate vibrations that contain a component of the dipole moment normal to the surface are active. Metals have large electrical conductivities at infrared frequencies, and the parallel electric field component goes to zero at the surface. Surface Raman spectroscopy (SRS) utilizes the visible region of the electromagnetic spectrum where metals are only moderate conductors; correspondingly, there are electric field gradients both perpendicular and parallel to the surface, with the perpendicular component being significantly stronger than the parallel.[6−8] Thus, vibrational modes that contain a component of the bond polarizability normal to the surface are more strongly enhanced, yet vibrations parallel to the surface can still be observed.

The surface site symmetry of an adsorbate can further complicate the interpretation of surface vibrational spectra.[9] This is of particular importance when studying centrosymmetric molecules because if the center of inversion is lost upon adsorption then both IR- and hyper-Raman-active modes may be observed in the Raman spectrum. There have been a series of surface-enhanced Raman scattering (SERS) studies on centrosymmetric adsorbates including benzene (D_{6h}),[10−18] pyrazine (D_{2h}),[13,18−27] and C_{60} (I_h).[16,28−33] In most of these reports, symmetry-forbidden modes were observed. For example, the SER spectra of benzene

† Part of the Electrochemistry special issue.

* Corresponding author. E-mail: vanduyne@chem.northwestern.edu.

(1) Chabal, Y. J. *Surf. Sci. Rep.* **1988**, *8*, 211−357.
(2) Fan, J. F.; Trenary, M. *Langmuir* **1994**, *10*, 3649−3657.
(3) Hollins, P. *Vacuum* **1994**, *45*, 705−714.
(4) Dumas, P. *Surf. Interface Anal.* **1994**, *22*, 561−567.
(5) Bradshaw, A. M.; Schweizer, E. In *Spectroscopy of Surfaces*; Clark, R. J. H., Hester, R. E., Eds.; John Wiley & Sons: New York, 1988; Vol. 16, p 413.
(6) Hallmark, V. M.; Campion, A. *J. Chem. Phys.* **1986**, *84*, 2933−2941.
(7) Moskovits, M. *J. Chem. Phys.* **1982**, *77*, 4408−4416.
(8) Creighton, J. A. In *Spectroscopy of Surfaces*; Clark, R. J. H., Hester, R. E., Eds.; John Wiley & Sons: New York, 1988; Vol. 15, p 37.
(9) Nichols, H.; Hexter, R. M. *J. Chem. Phys.* **1981**, *75*, 3126−3136.
(10) Moskovits, M.; Dilella, D. P. *J. Chem. Phys.* **1980**, *73*, 6068−6075.
(11) Gao, P.; Weaver, M. J. *J. Phys. Chem.* **1985**, *89*, 5040−5046.
(12) Wolkow, R. A.; Moskovits, M. *J. Chem. Phys.* **1986**, *84*, 5196−5199.
(13) Moskovits, M.; Dilella, D. P.; Maynard, K. J. *Langmuir* **1988**, *4*, 67−76.
(14) Gao, X. P.; Davies, J. P.; Weaver, M. J. *J. Phys. Chem.* **1990**, *94*, 6858−6864.
(15) Lund, P. A.; Smardzewski, R. R.; Tevault, D. E. *Chem. Phys. Lett.* **1982**, *89*, 508−510.
(16) Litorja, M.; Haynes, C. L.; Haes, A. J.; Jensen, T. R.; Van Duyne, R. P. *J. Phys. Chem. B* **2001**, *105*, 6907−6915.
(17) Howard, M. W.; Cooney, R. P. *Chem. Phys. Lett.* **1982**, *87*, 299−304.
(18) Li, X.-Y.; Huang, Q.-J.; Petrov, V. I.; Xie, Y.-T.; Luo, Q.; Yu, X.; Yan, Y.-J. *J. Raman Spectrosc.* **2005**, *36*, 555−573.
(19) Munizmiranda, M.; Neto, N.; Sbrana, G. *J. Mol. Struct.* **1986**, *143*, 275−278.
(20) Munizmiranda, M.; Neto, N.; Sbrana, G. *J. Phys. Chem.* **1988**, *92*, 954−959.
(21) Arenas, J. F.; Soto, J.; Tocon, I. L.; Fernandez, D. J.; Otero, J. C.; Marcos, J. I. *J. Chem. Phys.* **2002**, *116*, 7207−7216.
(22) Li, W. H.; Li, X. Y.; Yu, N. T. *Chem. Phys. Lett.* **1999**, *305*, 303−310.
(23) Brolo, A. G.; Irish, D. E. *J. Electroanal. Chem.* **1996**, *414*, 183−196.
(24) Arenas, J. F.; Woolley, M. S.; Tocon, I. L.; Otero, J. C.; Marcos, J. I. *J. Chem. Phys.* **2000**, *112*, 7669−7683.
(25) Soto, J.; Fernandez, D. J.; Centeno, S. P.; Tocon, I. L.; Otero, J. C. *Langmuir* **2002**, *18*, 3100−3104.
(26) Huang, Q. J.; Lin, X. F.; Yang, Z. L.; Hu, J. W.; Tian, Z. Q. *J. Electroanal. Chem.* **2004**, *563*, 121−131.
(27) Cui, L.; Liu, Z.; Duan, S.; Wu, D.-Y.; Ren, B.; Tian, Z.-Q.; Zou, S.-Z. *J. Phys. Chem. B* **2005**, *109*, 17597−17602.
(28) Akers, K. L.; Cousins, L. M.; Moskovits, M. *Chem. Phys. Lett.* **1992**, *190*, 614−620.
(29) Garrell, R. L.; Herne, T. M.; Szafranski, C. A.; Diederich, F.; Ettl, F.; Whetten, R. L. *J. Am. Chem. Soc.* **1991**, *113*, 6302−6303.

10.1021/la0612264 CCC: $33.50
Published on Web 09/12/2006

on cold-evaporated films contained the a_{2u} and e_{2u} vibrational modes, which are not Raman active for the free molecule (D_{6h}). If the site symmetry of benzene is reduced from D_{6h} to C_{3v} through adsorption at a 3-fold site, then the a_{2u} and e_{2u} modes transform as Raman-active modes.[10] Thus, molecular site symmetry reduction through surface adsorption can and has been used to describe the existence of forbidden bands in the SER spectra of centrosymmetric adsorbates.

However, various experimental observations such as large intensities of the normally forbidden bands and small shifts in frequency of the allowed modes have prompted a second explanation to account for these forbidden modes.[10] This second theory suggests that the centrosymmetric molecule retains its inversion symmetry upon adsorption yet on rough surfaces with features of a small radius of curvature both the field and the field gradient undergo enhancement and under certain circumstances may become equal. The dipole moment induced in a molecule is given by[10]

$$\mu_i = \alpha_{ij}E_j + \frac{1}{3}A_{ijk}\frac{\partial E_j}{\partial k} + G_{ij}B_j \qquad (1)$$

where i, j, and k may be x, y, and z. E_j and B_j are the j components of the electric and magnetic fields, and α_{ij}, A_{ijk}, and G_{ij} are components of the normal polarizability, the polarizability that produces a quadrupole moment proportional to the field, and the magnetic moment polarizability, respectively. The tensor **A** transforms precisely as the tensor **B** that gives rise to the hyper-Raman effect, but unlike **B**, **A** increases linearly with applied field strength. Therefore, if the field and field gradient have equal efficiency, then vibrational modes that are normally either Raman- or hyper-Raman-active will appear together in the SER spectrum. For benzene on cold-evaporated films, both the a_{2u} and e_{2u} modes are hyper-Raman-active and appear in SER spectra with an intensity equivalent to that of the gerade Raman-active modes. This field gradient mechanism can account for the strong intensity of these bands, whereas symmetry reduction would predict weaker scattering. Perry et al.[34] have shown that for molecules adsorbed on flat surfaces the field gradient mechanism is not important. However, more data is needed to directly correlate the degree to which the field gradient mechanism influences surface-enhanced vibrational spectra in general.

This article presents a detailed study of the electrochemical SEHR (ECHEM-SEHR) spectra of centrosymmetric molecules adsorbed on Ag electrodes. In this work, the SEHR spectra of *trans*-1,2-bis(4-pyridyl)ethylene (BPE) at different potentials (−0.2 to −1.1 V vs Ag/AgCl) are presented for the first time, and a reversible potential tuning of the SEHR spectra of BPE is demonstrated. The ECHEM-SEHR and SER spectra of BPE and 4,4′-bipyridine (BPY) in various electrochemical environments were studied to address two questions: (1) Which mechanism is more prevalent in dictating SER and SEHR spectra of centrosymmetric molecules, site symmetry reduction, or field gradient effects? (2) What type of molecular information can SEHRS provide that SERS cannot? By comparing the SEHRS and SERS vibrational frequencies and intensities of the same centrosymmetric molecule in the same environment, we can observe the operation of two different vibrational selection rules and gain insight into what factors govern surface-enhanced vibrational spectra. The results suggest that the field gradient mechanism does not contribute significantly to the spectra of the molecules used in this study. In addition, very few of the SEHRS modes undergo symmetry reduction whereas the majority of the BPE molecule retains its inversion symmetry when the potential is at a specific fixed value (i.e., $E = -0.7$ V vs Ag/AgCl). With regard to novel molecular information, we will show that SEHRS proves to be significantly more sensitive to local environmental changes than SERS. This is consistent with results obtained previously in SEHRS and SERS studies of pyrazine and pyridine.[18,22] More specifically, we have found that in the electrochemical environment SEHRS can detect changes in ΔG_{ads}, the free energy of adsorption by the adsorbate to the surface, and it can detect the presence of coadsorbed counterions, whereas the SER spectra are essentially insensitive to such effects.

The exquisite sensitivity that SEHRS shows for the local adsorption environment of the molecule may be of use in the investigation of the mechanism of single-molecule SERS (SMSERS). Since the first observation of SMSERS in 1997,[35,36] intense interest has been generated as to the mechanism of the enormous enhancement factors (10^{14}) present in the effect. The large enhancements are seen only with certain "hot" metal particles. It has been postulated by Michaels et al.[37,38] that the enhanced electromagnetic fields making possible SMSERS are located in junctions between nanoparticles. Because the precise conditions that give rise to SMSERS remain an area of vigorous research, SEHRS may have the ability to make a contribution to this exciting investigation.

Ag film over nanosphere (FON) electrodes,[39,40] which have well-defined nanostructure morphology, were used as the SERS-active substrate in these studies. The surface roughness produced by vapor deposition of a SERS-active metal on top of a nanosphere monolayer is extremely reproducible. In particular, these surfaces are useful for SERS studies under electrochemical conditions because they do not depend on adsorbed halide anions during SERS-active generation. Therefore, new SERS experiments can be carried out with metal FON electrodes that were previously not possible with metal oxidation−reduction cycle (MORC) roughened electrodes. For example, the use of metal FON electrodes enables a variation of the concentration or chemical nature of the supporting electrolyte in an electrochemical SERS experiment.

Experimental Methods

Both *trans*-1,2-bis(4-pyridyl)ethylene (BPE) and 4,4′-bipyridine (BPY) were purchased from Aldrich, recrystallized twice from methanol/water, and sublimed. Water was obtained from a Millipore water filtration system (18.2 MΩ cm^{-1}). All solutions were 0.4 mM BPE and 1.0 mM BPY with the supporting electrolyte concentration and identity described in the text. KCl, KBr, and $KClO_4$ were purchased from Mallinckrodt. Ag (99.99%) was purchased from D. F. Goldsmith (Evanston, IL), and tungsten vapor deposition boats were purchased from R. D. Mathis (Long Beach, CA). Polystyrene

(30) Liu, J. Q.; Zhao, T. N.; Mo, Y. J.; Li, T. X.; Liu, Y. L.; Zhu, K.; Li, Y. L.; Yao, Y. X.; Yang, D. L.; Wang, X. H.; Zhu, D. B. *Solid State Commun.* **1992**, *81*, 757−760.
(31) Zhang, Y.; Edens, G.; Weaver, M. J. *J. Am. Chem. Soc.* **1991**, *113*, 9395−9397.
(32) Siu, G. G.; Liu, Y. L.; Xie, S. S.; Xu, J. M.; Li, T. K.; Xu, L. G. *Thin Solid Films* **1996**, *274*, 147−149.
(33) Yang, X. C.; Fang, Y. *J. Phys. Chem. B* **2003**, *107*, 10100−10103.
(34) Perry, S. S.; Hatch, S. R.; Campion, A. *J. Chem. Phys.* **1996**, *104*, 6856−6859.
(35) Nie, S. M.; Emery, S. R. *Science* **1997**, *275*, 1102−1106.
(36) Kneipp, K.; Wang, Y.; Kneipp, H.; Perelman, L. T.; Itzkan, I.; Dasari, R.; Feld, M. S. *Phys. Rev. Lett.* **1997**, *78*, 1667−1670.
(37) Michaels, A. M.; Nirmal, M.; Brus, L. E. *J. Am. Chem. Soc.* **1999**, *121*, 9932−9939.
(38) Michaels, A. M.; Jiang, J.; Brus, L. *J. Phys. Chem. B* **2000**, *104*, 11965−11971.
(39) Vanduyne, R. P.; Hulteen, J. C.; Treichel, D. A. *J. Chem. Phys.* **1993**, *99*, 2101−2115.
(40) Dick, L. A.; McFarland, A. D.; Haynes, C. L.; Van Duyne, R. P. *J. Phys. Chem. B* **2002**, *106*, 853−860.

nanospheres, diameter = 542 ± 7 nm, with a terminal carboxyl functional group were purchased from IDC (Portland, OR) and were diluted 1:1 by volume with a solution of the surfactant Triton X-100 (Aldrich) and methanol (1:400 by volume) to promote a close-packing arrangement.

AgFON electrodes were prepared by spin coating a monolayer of the polystyrene nanospheres onto a Ag disk electrode (diameter = 5 mm) using a spin coater designed in-house. The Ag disk electrode consisted of a Ag rod sealed with epoxy (Torr Seal, Varian) into a Teflon frame. The electrode was then placed in a modified Consolidated Vacuum Corporation vapor deposition system[41] with a base pressure of 10^{-7} Torr. A 200 nm Ag film was deposited over the nanospheres by thermal vapor deposition from a tungsten boat at a rate of 0.3−0.4 nm s^{-1}. The electrode temperature remained <50 °C, and the chamber pressure was always $<10^{-6}$ Torr during the deposition. Mass thickness was measured with an in-house-designed quartz-crystal microbalance calibrated by both cyclic voltammetry and STM. The spectroelectrochemical cell was designed in-house, and all potentials are reported with respect to a Ag/AgCl reference electrode.[39]

A Spectra Physics Series CW mode-locked 3000 Nd:YAG laser was used for λ_{ex} = 1064 and 532 nm. Both SEHR and SER spectra were obtained on an ACTON VM-505 (Acton, MA) single-grating monochromator equipped with a Photometrics PM-512 CCD detector (Tucson, AZ). A Physical Optics Co. (Torrance, CA) holographic edge filter was used for the rejection of λ_{ex} in SERS experiments, whereas Schott glass filter 59062 was used to reject λ_{ex} in SEHRS experiments. The angle of incidence of the laser excitation source was 45° with respect to the surface normal, and scattered light was collected parallel to the surface normal with *f*/1 optics. In all spectra, the laser source was spot focused to ca. 100 μm in diameter. The laser powers used were as follows: 1.0 W for SEHRS and 10 mW for SERS. To measure the normal Raman scattering of the solid samples, 30 mW was used for BPE, and 35 mW was used for BPY.

Results and Discussion

A. Site Symmetry Reduction vs Field Gradient Mechanism. Figure 1 shows the SEHR (Figure 1A) and SER (Figure 1B) spectra of BPE adsorbed to a AgFON electrode at a fixed potential, $E = -0.7$ V vs Ag/AgCl. This potential was chosen because it was the potential that gave the strongest and most unique SEHR spectrum for BPE. A complete vibrational assignment of the BPE SER spectra based upon ab initio calculations of the normal modes has been published.[42] There are numerous differences between the SEHR and SER spectra. There are peaks in the SER spectrum that are not duplicated in the SEHR spectrum (i.e., 1640 cm^{-1}). In addition, some peaks present in the SEHR spectrum are not present in the SER spectrum (i.e., 1526, 1473, and 550 cm^{-1}). Also, whereas many modes of these two spectra have similar locations, they do not share identical frequencies or relative intensities.

BPE is a centrosymmetric molecule with C_{2h} symmetry. As such, its hyper-Raman and Raman-active modes are complementary. If site symmetry reduction were to occur upon surface adsorption, then BPE adsorbed in a flat orientation with the pyridine rings parallel to the surface would have C_{2v} symmetry and an end-on adsorption involving a single nitrogen would result in C_s symmetry (Figure 2). On the basis of the correlation diagram in Figure 2, either of these symmetry reductions would transform all of the vibrational modes of BPE as both Raman- and hyper-Raman-allowed. In such a circumstance, the SERS and SEHRS vibrational bands should be identical in frequency although the relative intensity distribution would be quite different as in the published case of pyridine (C_{2v}) on Ag.[22,43] Figure 1 clearly shows that this is not happening in this case. For example, the SERS peak at 1640 cm^{-1} (Figure 1B) that is attributed to the central ethylene C═C stretch is Raman-active and not hyper-Raman-active (i.e., gerade symmetry only) according to literature theoretical predictions for this C_{2h} molecule.[42] The absence of this intense SERS peak in the SEHR spectrum strongly implies that little or no symmetry reduction occurs upon adsorption. Also, the SEHRS band at 1592 cm^{-1} (Figure 1A) is not the same vibrational mode as the SERS band at 1604 cm^{-1} (Figure 1B). Although both are ring-stretching modes, they have different symmetry resulting in two separate frequency values. It does appear that at least two modes of BPE are altered by surface interactions. Between 1450 and 1550 cm^{-1}, there should be two gerade and two ungerade vibrational modes that involve a displacement of the nitrogen position.[42] There are two SERS bands (1544 and 1493 cm^{-1}) in this region, but there are four present in the SEHR spectrum (1548, 1526, 1489, and

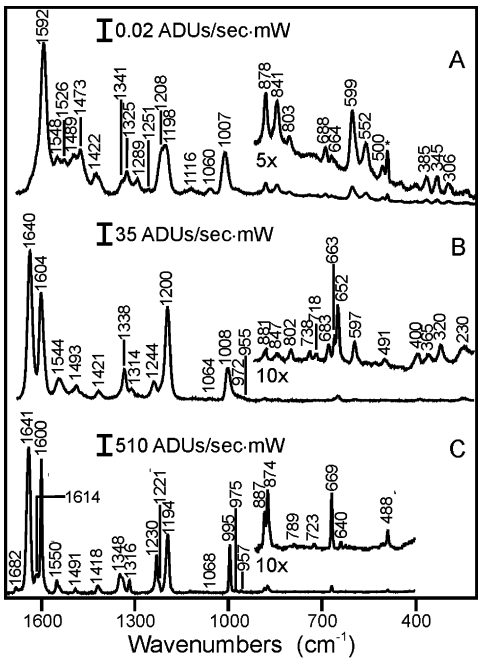

Figure 1. Vibrational spectra of BPE. (A) SEHR spectrum on a AgFON electrode with $[Cl^-] = 0.1$ M at a fixed potential $E = -0.7$ V and 1.0 W of $\lambda_{ex} = 1064$ nm, 300 s integration. (B) SER spectrum on a AgFON electrode with $[Cl^-] = 0.1$ M at a fixed potential $E = -0.7$ V and 10 mW of $\lambda_{ex} = 532$ nm, 30 s integration. (C) NRS of the solid with 30 mW of $\lambda_{ex} = 532$ nm, 1 s integration. The (*) indicates a Hg line from stray room light.

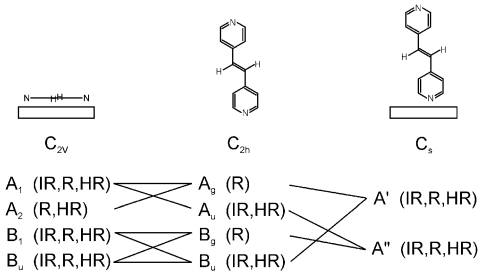

Figure 2. Correlation diagram illustrating the two different adsorption orientations for BPE and their respective site symmetry reduction. The modes are classified as either infrared (IR)-, Raman (R)-, or hyper-Raman (HR)-active.

(41) Hulteen, J. C.; Vanduyne, R. P. *J. Vac. Sci. Technol., A* **1995**, *13*, 1553−1558.

(42) Yang, W. H.; Hulteen, J.; Schatz, G. C.; VanDuyne, R. P. *J. Chem. Phys.* **1996**, *104*, 4313−4323.

(43) Golab, J. T.; Sprague, J. R.; Carron, K. T.; Schatz, G. C.; Vanduyne, R. P. *J. Chem. Phys.* **1988**, *88*, 7942−7951.

1473 cm^{-1}). This suggests that whereas a majority of the BPE SEHR spectrum shows symmetry retention these two modes involving motion near the Ag surface show site reduction. If BPE adsorbs end-on, then the two nitrogens are in different environments resulting in two different observed frequencies. The absence of this reduction in the SERS implies that SEHRS may be more sensitive to the surface environment.

Unlike site symmetry reduction, the field gradient mechanism predicts that the centrosymmetric symmetry of BPE will be retained upon adsorption and hyper-Raman band frequencies should coexist within the SER spectra because of the intense electric field gradients present near the metal surface.[44] The data in Figure 1 suggests that this process does not significantly contribute to spectra collected from AgFON electrodes. For example, in Figure 1A the 1592 cm^{-1} ring mode is the strongest band in the SEHR spectrum, yet the associated SER spectrum (Figure 1B) does not show any evidence of peak intensity at that location. This disparity would not exist if the field gradient mechanism were operational. Although the absence of peaks cannot be used to disprove a theory, it can imply the insignificance of its contribution.

In previous literature studies, the presence of new peaks in a SER spectrum with respect to NRS has been used to suggest the presence of field gradient effects. Therefore, the NR spectrum of BPE is also reported (Figure 1C). With the exception of some weak low-frequency modes that may not have been well resolved in the NRS, there are essentially no new peaks in the SER spectra of BPE versus the NRS. This further suggests that field gradient effects are very weak on AgFON electrodes if they are present at all.

If field gradient models do not apply very strongly to this system and site symmetry reduction applies to very few modes, then BPE must retain most of its free molecule centrosymmetry upon adsorption on a AgFON at a fixed potential, $E = -0.7$ V. Thus, SEHRS is capable of probing a completely different set of vibrational modes, namely, ungerade vibrations. Although such a suggestion is not rigorously correct (i.e., geometrical arguments dictate that inversion symmetry must be lost upon surface contact), the spectroscopic evidence does demonstrate that the inversion symmetry of BPE is significantly retained.

B. Potential-Induced Spectral Modulations. To determine if this apparent symmetry retention of BPE was a stable configuration, the potential of the AgFON electrode was tuned positive from −0.7 to −0.3 V. Within this potential range, no net electrochemistry was detected, yet a series of fully reversible changes in the SEHR spectra were recorded. However, the SER spectra were found to be independent of potential. Figures 3−11 show detailed, high-resolution comparisons between the SEHR and SER spectra of BPE at −0.7, −0.5, and −0.3 V in various spectral regions. The following changes in the SEHR spectra were observed within these potential excursions: (1) peak shifts, (2) changes in the ffwhm, (3) loss or gain of peaks, and (4) changes in relative intensities. Table 1 summarizes all of the observed SEHRS and SERS vibrational frequencies for BPE and the associated potential-dependent changes at the three different potentials used in Figures 3−11. All terminology is established via a scan toward positive potentials. For example, a peak gain is defined as a peak that appears in the spectra at a more positive potential, −0.3 V, but is absent at −0.7 V. The potential-induced SEHR spectral changes are not due to laser-induced damage or nonlinear surface photochemistry because all effects are fully reversible.

(44) Sass, J. K.; Neff, H.; Moskovits, M.; Holloway, S. *J. Phys. Chem.* **1981**, *85*, 621−623.

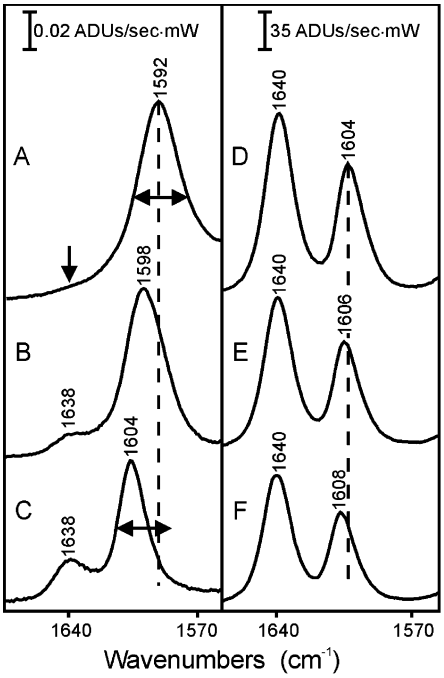

Figure 3. Potential dependence of the SEHR and SER spectra of BPE on a AgFON electrode with $[Cl^-] = 0.1$ M in the 1670−1560 cm^{-1} spectral region. SEHRS: (A) −0.7, (B) −0.5, and (C) −0.3 V. SERS: (D) −0.7, (E) −0.5, and (F) −0.3 V. Same acquisition parameters as in Figure 1. The dotted line indicates a peak shift, the horizontal line indicates a fwhm change, and a downward-facing arrow indicates a peak gain at more positive potentials.

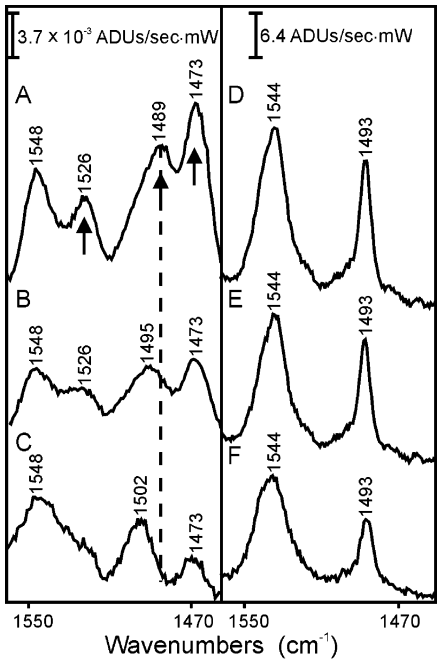

Figure 4. Potential dependence of the SEHR and SER spectra of BPE on a AgFON electrode with $[Cl^-] = 0.1$ M in the 1560−1460 cm^{-1} spectral region. SEHRS: (A) −0.7, (B) −0.5, and (C) −0.3 V. SERS: (D) −0.7, (E) −0.5, and (F) −0.3 V. Same acquisition parameters as in Figure 1. The upward-facing arrow indicates a peak loss at more positive potentials.

Figure 3 gives examples of the first three types of changes upon application of this potential excursion. The 1592 cm^{-1} SEHRS band shifts 12 cm^{-1}, yet the 1604 cm^{-1} SERS band shifts only 4 cm^{-1}. The fwhm of the SEHRS 1592 cm^{-1} band decreases from 30 to 17 cm^{-1} with no associated changes in the

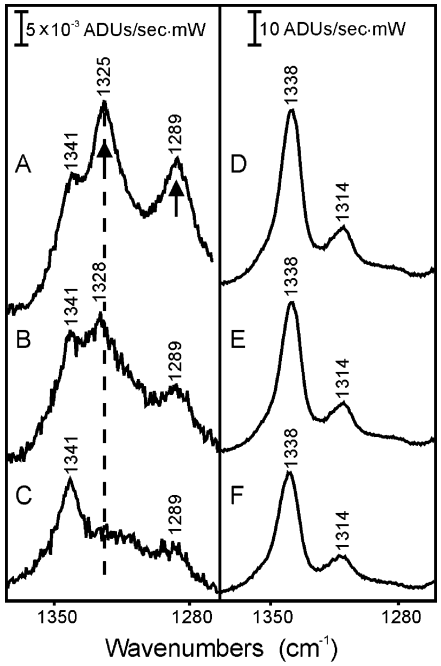

Figure 5. Potential dependence of the SEHR and SER spectra of BPE on a AgFON electrode with $[Cl^-] = 0.1$ M in the 1370−1260 cm^{-1} spectral region. SEHRS: (A) −0.7, (B) −0.5, and (C) −0.3 V. SERS: (D) −0.7, (E) −0.5, and (F) −0.3 V. Same acquisition parameters as in Figure 1.

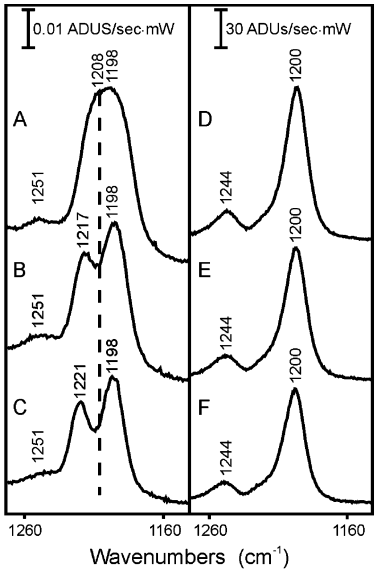

Figure 6. Potential dependence of the SEHR and SER spectra of BPE on a AgFON electrode with $[Cl^-] = 0.1$ M in the 1270−1150 cm^{-1} spectral region. SEHRS: (A) −0.7, (B) −0.5, and (C) −0.3 V. SERS: (D) −0.7, (E) −0.5, and (F) −0.3 V. Same acquisition parameters as in Figure 1.

1604 cm^{-1} SERS mode. Also, a SEHRS band at 1638 cm^{-1} appears and gains intensity as the voltage reaches −0.3 V. As previously stated, the 1638 cm^{-1} band has gerade symmetry only and should not be hyper-Raman-active. However, at more positive potentials only, this band appears in the SEHR spectrum, implying that the site symmetry of BPE may be reduced as a result of potential tuning.

In the SEHR spectra in Figure 4, there are also three types of changes. The 1489 and 1473 cm^{-1} bands decrease in relative intensity, the 1526 cm^{-1} band disappears, and the 1489 cm^{-1} band shifts 13 cm^{-1}. However, there are no changes in the SER

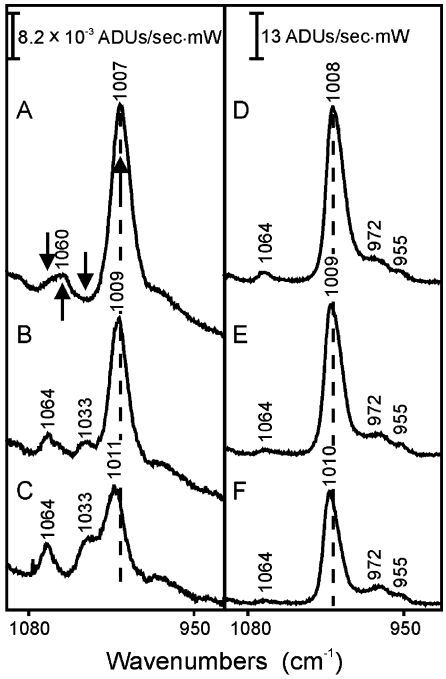

Figure 7. Potential dependence of the SEHR and SER spectra of BPE on a AgFON electrode with $[Cl^-] = 0.1$ M in the 1090−935 cm^{-1} spectral region. SEHRS: (A) −0.7, (B) −0.5, and (C) −0.3 V. SERS: (D) −0.7, (E) −0.5, and (F) −0.3 V. Same acquisition parameters as in Figure 1.

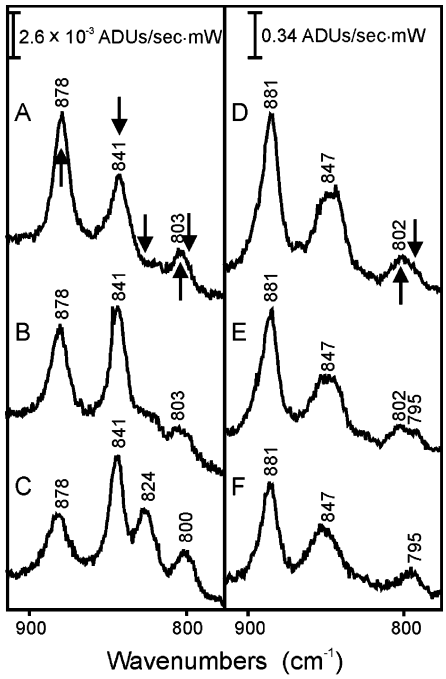

Figure 8. Potential dependence of the SEHR and SER spectra of BPE on a AgFON electrode with $[Cl^-] = 0.1$ M in the 920−880 cm^{-1} spectral region. SEHRS: (A) −0.7, (B) −0.5, and (C) −0.3 V. SERS: (D) −0.7, (E) −0.5, and (F) −0.3 V. Same acquisition parameters as in Figure 1 except for (D−F) 20 mW and 120 s integration.

spectra. Figures 5−11 continue to show various examples of the different types of changes in the SEHR spectra in all frequency regions whereas little or no changes are observed in the SERS.

We have considered four possible mechanisms as to the origin of this reversible potential tuning of the SEHRS of BPE, and they are schematically depicted in Figure 12. They are an adsorbate

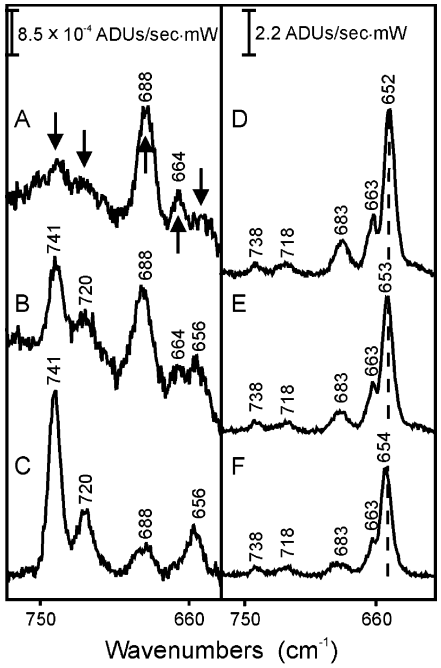

Figure 9. Potential dependence of the SEHR and SER spectra of BPE on a AgFON electrode with $[Cl^-] = 0.1$ M in the 770−640 cm^{-1} spectral region. SEHRS: (A) −0.7, (B) −0.5, and (C) −0.3 V. SERS: (D) −0.7, (E) −0.5, and (F) −0.3 V. Same acquisition parameters as in Figure 1 except for (A−C) 600 s integration.

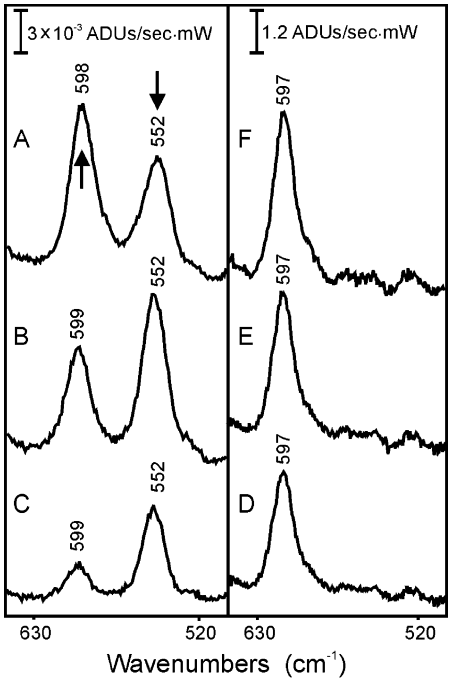

Figure 10. Potential dependence of the SEHR and SER spectra of BPE on a AgFON electrode with $[Cl^-] = 0.1$ M in the 640−510 cm^{-1} spectral region. SEHRS: (A) −0.7, (B) −0.5, and (C) −0.3 V. SERS: (D) −0.7, (E) −0.5, and (F) −0.3 V. Same acquisition parameters as in Figure 1.

orientation change, nanostructure bridging, a strong versus weak surface-molecule bond, and coadsorbed counterion effects.

A molecular reorientation such as that in Figure 12A could account for this potential-tuned data without invoking symmetry retention/reduction arguments. However, if BPE were undergoing a surface orientation change, then differences in relative intensity would be manifest within the SER spectrum as well as in the SEHRS because of the surface selection rule where vibrations

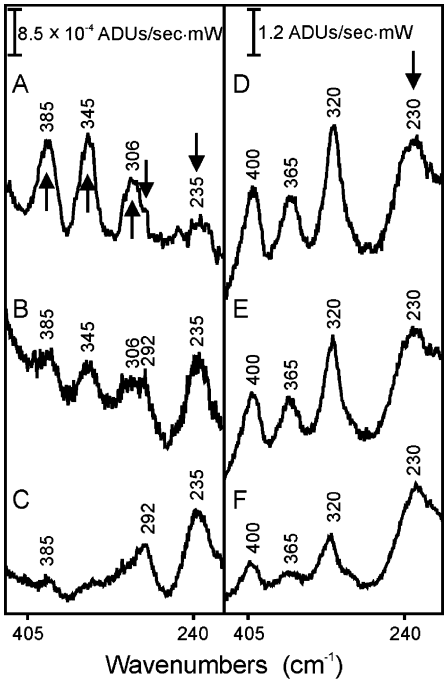

Figure 11. Potential dependence of the SEHR and SER spectra of BPE on a AgFON electrode with $[Cl^-] = 0.1$ M in the 415−220 cm^{-1} spectral region. SEHRS: (A) −0.7, (B) −0.5, and (C) −0.3 V. SERS: (D) −0.7, (E) −0.5, and (F) −0.3 V. Same acquisition parameters as in Figure 1.

normal to the surface are preferentially enhanced. This has been shown in numerous literature SERS studies.[11,25,45−50] Because no relative intensity changes exist in the SER spectra within the potential window employed, it is assumed that there is not a significant change in the angle of BPE with respect to the surface normal. The specific orientation of BPE is assumed to be end-on adsorption based upon thin-layer optical absorption measurements by Gui et al.[51] on Pt as well as experiments by McMahon et al.,[52] which determined that BPE must absorb end-on on electrochemically roughened Ag because of alignment characteristics required for the photochemical products that they observed. The theoretical calculations made by Yang et al.[42] support the conclusion that the BPE molecule is adsorbed end-on to the AgFON electrode with an orientation normal to the electrode surface.

The nanostructure bridging model in Figure 12B describes two distinct adsorption sites for BPE on the AgFON: (i) a monodentate site in which one nitrogen binds to the surface, which would reduce the site symmetry of BPE to C_s, resulting in the appearance of the 1638 cm^{-1} SEHRS band and (ii) a bidentate bridging site at which BPE binds via both nitrogen atoms at defect sites within the surface substructure, which would retain the inversion symmetry of BPE, resulting in the absence of the 1638 cm^{-1} SEHRS band. At −0.3 V, both sites would be occupied, and upon a potential excursion to −0.7 V, only the

(45) Moskovits, M.; Suh, J. S. *J. Phys. Chem.* **1988**, *92*, 6327−6329.
(46) Itoh, K.; Minami, K.; Tsujino, T.; Kim, M. *J. Phys. Chem.* **1991**, *95*, 1339−1345.
(47) Bukowska, J.; Calvo, M.; Jurkiewicz-Herbich, M.; Jackowska, K. *Pol. J. Chem.* **2002**, *76*, 1151−1162.
(48) Cao, P.; Yao, J. L.; Ren, B.; Gu, R.; Tian, Z. Q. *J. Phys. Chem. B* **2002**, *106*, 7283−7285.
(49) Gu, R. A.; Cao, P. G.; Yao, J. L.; Ren, B.; Xie, Y.; Mao, B. W.; Tian, Z. Q. *J. Electroanal. Chem.* **2001**, *505*, 95−99.
(50) Dick, L. A.; Haes, A. J.; Van Duyne, R. P. *J. Phys. Chem. B* **2000**, *104*, 11752−11762.
(51) Gui, Y. P.; Porter, M. D.; Kuwana, T. *Anal. Chem.* **1985**, *57*, 1474−1476.
(52) McMahon, J. J.; Dougherty, T. P.; Riley, D. J.; Babcock, G. T.; Carter, R. L. *Surf. Sci.* **1985**, *158*, 381−392.

Table 1. SEHRS and SERS Vibrational Frequencies at Various Applied Potentials vs Ag/AgCl for BPE at λ_{ex} = 1064 and 532 nm, Respectively[a]

	SEHRS				SERS		
trend	−0.3 V	−0.5 V	−0.7 V	trend	−0.3 V	−0.5 V	−0.7 V
G	1638	1638			1640	1640	1640
S, W	1604	1598	1592	S	1608	1606	1604
	1548	1548	1548		1544	1544	1544
L		1526	1526				
S	1502	1495	1489		1493	1493	1493
I	1473	1473	1473				
	1422	1422	1422		1421	1421	1421
	1341	1341	1341		1338	1338	1338
S, L		1328	1325		1314	1314	1314
I	1289	1289	1289				
	1251	1251	1251		1244	1244	1244
S	1221	1217	1208				
	1198	1198	1198		1200	1200	1200
	1116	1116	1116				
G	1064	1064			1064	1064	1064
L		1060	1060				
G	1033	1033					
S	1011	1009	1007	S	1010	1009	1008
					972	972	972
					955	955	955
I	878	878	878		881	881	881
	841	841	841		847	847	847
G	824						
	800	803	803	L		802	802
				G	795	795	
G	741	741			738	738	738
G	720	720			718	718	718
I	688	688	688		683	683	683
L		664	664		663	663	663
G	656	656		S	654	653	652
I	599	599	599		597	597	597
D	552	552	552				
I	500	500	500		491	491	491
	385	385	385		400	400	400
L		345	345		365	365	365
L		306	306		320	320	
G	292	292					320
G	235	235	235	D	230	230	
D							230

[a] S = peak position shift; W = change in fwhm of peak; L = loss of peak; G = gain of peak; D = decrease in relative band intensity; I = increase in relative band intensity.

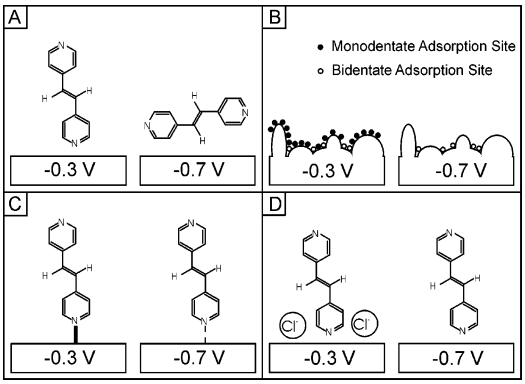

Figure 12. Schematic illustration of four scenarios that could result in the potential-tuned SEHR spectra of BPE. (A) Orientation change of the molecule with respect to the surface normal. (B) Nanostructure bridging. (C) Strong vs weak surface−molecule bond, and (D) counterion coadsorption.

bidentate sites would be occupied. Because of the AgFON surface morphology, a very small percentage of the total surface area could contain these bidentate sites. The strong intensity modulations in both the SEHR and SER spectra that would be expected

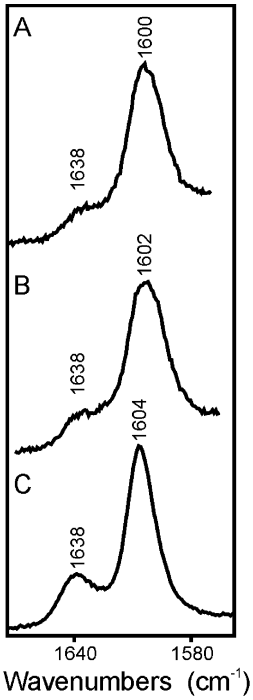

Figure 13. SEHRS of BPE with different [Cl⁻] at a fixed potential $E = -0.3$ V in the 1670−1560 cm^{-1} spectral region where $R = I(1600\ \text{cm}^{-1})/I(1638\ \text{cm}^{-1})$. (A) [Cl⁻] = 1.0×10^{-3} M, $R = 39$; (B) [Cl⁻] = 0.0100 M, $R = 19$; and (C) [Cl⁻] = 0.1000 M, $R = 7$. Same acquisition parameters as in Figure 1B.

with potential excursions under this model were not observed. Therefore, bidentate bridging sites for BPE adsorption did not play a role in the potential-induced spectral variations for SEHRS of BPE.

Figure 12C depicts strong monodentate binding of BPE at more positive potentials and weaker binding at more negative potentials. This would produce bound BPE that was effectively C_{2h} at negative potentials but at more positive potentials would approach C_s. Literature studies of the adsorption of pyridine on Ag and Au are consistent with stronger ΔG_{ads} for potentials positive of the point of zero charge (pzc = −0.7 V vs SCE for Ag in aqueous Cl⁻) and weaker ΔG_{ads} for potentials negative of the pzc.[53] Such a model could account for some of the observed SEHR spectral changes for BPE, but changes might be expected in the SER spectra as well. There are, in fact, small shifts in some SERS-active modes of BPE (i.e., 1608, 1010, and 654 cm^{-1}; Table 1). If this modulating adsorption strength model is at least partially responsible for these spectral changes, then this suggests that SEHRS is significantly more sensitive to changes in local surface binding interactions than is SERS.

In the counterion coadsorption model shown as in Figure 12D, the presence of the anion coadsorbed on the AgFON surface may alter the symmetry of the adsorbed molecule by altering the local surface environment. If this phenomenon were operative, then one would expect to see a strong anion dependence in the SEHRS. Figure 13 shows the dependence of the SEHRS signal at different bulk Cl⁻ concentrations and a fixed potential $E = -0.3$ V in the 1600 cm^{-1} spectral region, where the 1638 cm^{-1} gerade mode has been shown to appear in the BPE SEHR spectrum. As the bulk Cl⁻ concentration increases from 1.0×10^{-3} M (Figure 13A) to 0.0100 M (Figure 13B) to 0.1000 M (Figure 13C), the SEHRS intensity ratio, I_{1600}/I_{1638}, decreases from 39 to 19 to 7, respectively. The relative increase of the 1638

(53) Zelenay, P.; Ricejackson, L. M.; Wieckowski, A. *Langmuir* **1990**, *6*, 974−979.

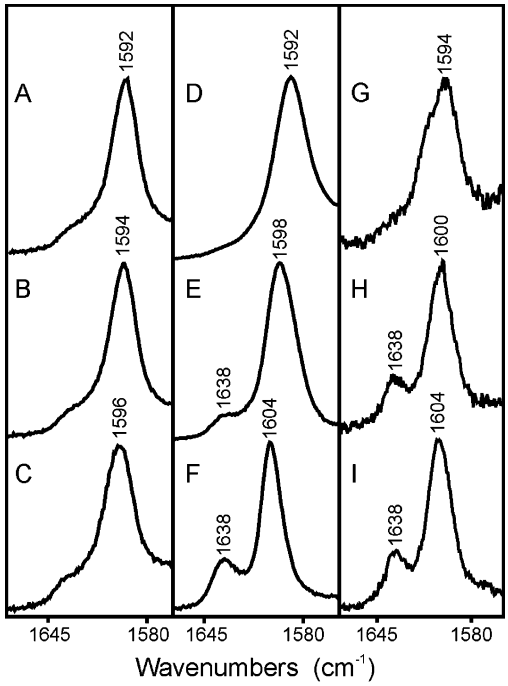

Figure 14. SEHRS of BPE with different counterions at different applied potentials in the 1670−1560 cm^{-1} spectral region. [ClO_4^-] = 0.1 M: (A) −0.7, (B) −0.5, and (C) −0.2 V. [Cl^-] = 0.1 M: (D) −0.7, (E) −0.5, and (F) −0.3 V. [Br^-] = 0.1 M: (G) −1.1, (H) −0.9, and (I) −0.7 V. Same acquisition parameters as in Figure 1B.

cm^{-1} gerade mode seen here strongly suggests that a higher surface concentration of the counterion causes a larger perturbation and reduction of the local symmetry of the adsorbate. Such an experiment was impossible to perform prior to the development of metal FON electrodes because oxidation−reduction cycle (ORC) roughening is strongly dependent on the composition of the supporting electrolyte. The deconvolution of the dependence of an ORC and the dependence of SEHRS intensities on the counterion cannot be accomplished with any certainty. However, AgFON electrodes are created ex-situ, and we are able to observe counterion effects on spectral characteristics that are independent of surface roughness.

The effects of counterion coadsorption on SEHR spectra were further tested by varying the electrolyte species instead of the concentration. The surface concentration of specifically adsorbed anions on Ag increases in the order $X^- = ClO_4^- < Cl^- < Br^-$ at a given applied potential,[54,55] and the potential-induced surface desorption of each anion occurs in the opposite order (i.e., Br^- desorbs from Ag at further negative potentials than that for Cl^-). If the counterion coadsorption model were operative, then one would expect to see different potential-dependent SEHRS behavior for each anion. Figure 14 shows the dependence of the BPE SEHRS signal on different coadsorbed anions at different potentials in the 1600 cm^{-1} spectral region. In Figure 14A−C, $X^- = ClO_4^-$ and $E = -0.7$, −0.5, and −0.2 V, respectively. The ethylene C═C stretch at 1638 cm^{-1} is essentially absent at all potentials because ClO_4^- does not have a significant surface concentration within this potential region. Figure 14D−F is identical to Figure 3A−C where $X^- = Cl^-$, and the 1638 cm^{-1} band is present at −0.3 V but disappears by −0.7 V. In Figure 14G−I, $X^- = Br^-$ and $E = -1.1$, −0.9, and −0.7 V, respectively. The 1638 cm^{-1} band does not disappear until −1.1 V, which is much further negative than was observed for Cl^-. The fact that there is different potential-dependent SEHRS behavior for the different anions further demonstrates that the presence of coadsorbed counterions does have an influence on the SEHR spectrum.

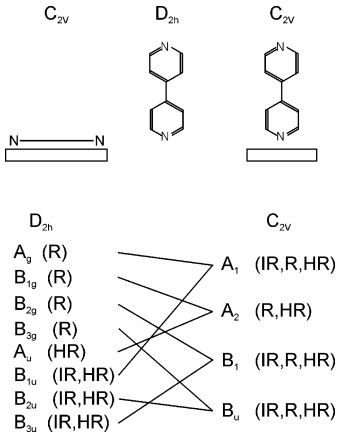

Figure 15. Correlation diagram illustrating the two different adsorption orientations for BPY and their respective site symmetry reductions. The modes are classified as either infrared (IR)-, Raman (R)-, or hyper-Raman (HR)-active.

From the SEHRS results of different anion concentrations and the potential dependence of different anions, it appears that coadsorbed counterions do lower the effective site symmetry of BPE, resulting in SEHR spectral changes. This mechanism has clearly been shown to be important whereas the orientation change and nanostructure bridging mechanisms have been shown not to play significant roles. In addition to the coadsorbed counterion effects, changes in ΔG_{ads} must be included as a possible contributor to these potential tuning effects because the influence of ΔG_{ads} has been neither proved nor disproved. Another result that should be stressed is that whereas SEHRS is very sensitive to these changes in the local adsorption environment SERS appears to be rather insensitive to them.

C. Different Molecule, Different ΔG_{ads}. This section attempts to further elucidate to what extent ΔG_{ads} contributes to the potential-induced SEHR spectral changes through the study of another centrosymmetric molecule, BPY. BPY was chosen because it has a similar structure to that of BPE but with D_{2h} symmetry that reduces to C_{2v} if adsorbed either end-on or parallel to the surface (correlation diagram, Figure 15).

Figure 16 shows the SEHR (Figure 16A) and SER (Figure 16B) spectra of BPY adsorbed to a AgFON electrode at a fixed potential, $E = -0.7$ V, and as expected, there are some differences between these spectra. Peaks are missing in the SEHRS that are present in the SERS (i.e., 1635 and 1515 cm^{-1}), and peaks with similar locations do not share identical frequencies or relative intensities. Because all bands in both spectra are not at equivalent frequencies, the symmetry of BPY is not significantly lowered upon adsorption, as was seen for BPE. With regard to field gradient effects, there are no new SERS bands (Figure 14B) as compared to the NRS (Figure 16C), suggesting a limited influence of this effect.

A potential excursion between −0.7 and −0.3 V resulted in very few changes in either the SEHR or SER spectra of BPY, unlike in the BPE studies. However, at −0.05 V a band at 1635 cm^{-1} appears in the SEHR spectra (Figure 17). Also in this region, the fwhm of the 1603 cm^{-1} SEHRS band decreases from 31 cm^{-1} at −0.7 V (Figure 17A) to 22 cm^{-1} at −0.3 V (Figure 17B) with no apparent changes in the SERS band at 1607 cm^{-1}. Peak shifts are present in this region as well. The 1603 cm^{-1}

(54) Bockris, J. O. M.; Paik, W.-K.; Genshaw, M. A. *J. Phys. Chem.* **1970**, *74*, 4266−75.
(55) Hupp, J. T.; Larkin, D.; Weaver, M. J. *Surf. Sci.* **1983**, *125*, 429−451.

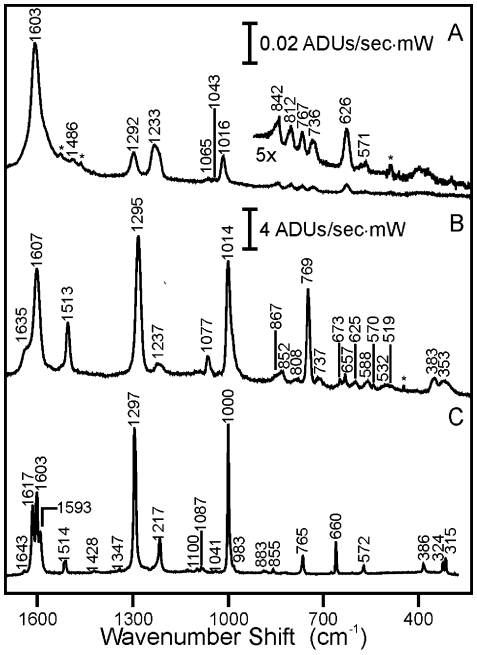

Figure 16. Vibrational spectra of BPY. (A) SEHR spectrum on a AgFON electrode with $[Cl^-] = 0.1$ M at a fixed potential $E = -0.7$ V and 1.0 W of $\lambda_{ex} = 1064$ nm, 300 s integration. (B) SER spectrum on a AgFON electrode with $[Cl^-] = 0.1$ M at a fixed potential $E = -0.7$ V and 10 mW of $\lambda_{ex} = 532$ nm, 150 s integration. (C) NRS of the solid with 35 mW of $\lambda_{ex} = 532$ nm, 1 s integration.

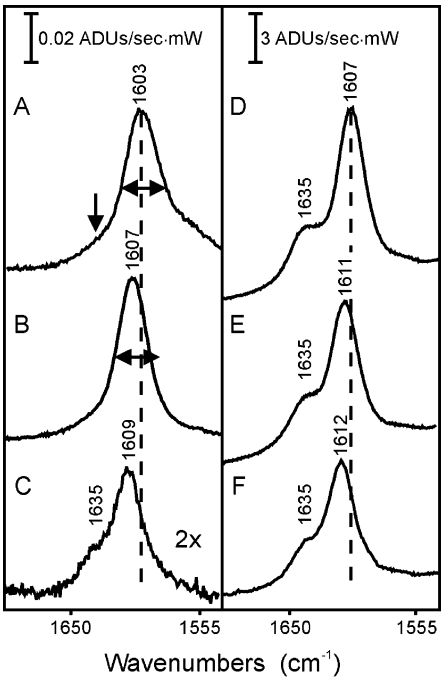

Figure 17. Potential dependence of the SEHR and SER spectra of BPY on a AgFON electrode with $[Cl^-] = 0.1$ M in the 1670−1545 cm^{-1} spectral region. SEHRS: (A) −0.7, (B) −0.3, and (C) −0.05 V. SERS: (D) −0.7, (E) −0.3, and (F) −0.05 V. Same acquisition parameters as in Figure 16.

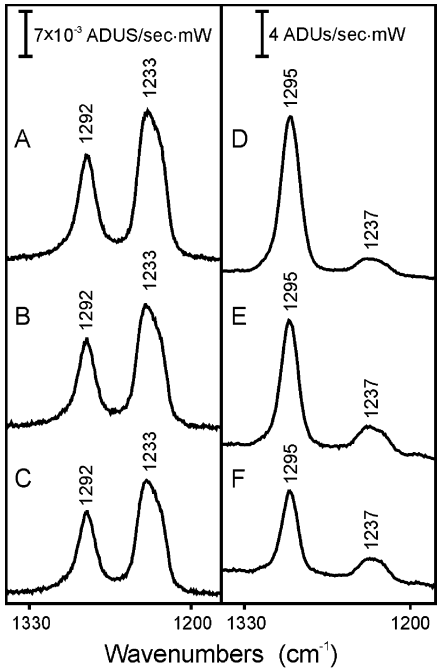

Figure 18. Potential dependence of the SEHR and SER spectra of BPY on a AgFON electrode with $[Cl^-] = 0.1$ M in the 1340−1190 cm^{-1} spectral region. SEHRS: (A) −0.7, (B) −0.5, and (C) −0.3 V. SERS: (D) −0.7, (E) −0.5, and (F) −0.3 V. Same acquisition parameters as in Figure 16 except for (D−F) 100 s integration.

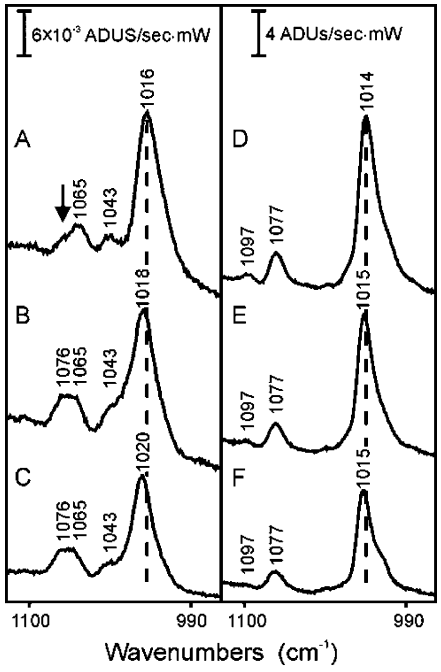

Figure 19. Potential dependence of the SEHR and SER spectra of BPY on a AgFON electrode with $[Cl^-] = 0.1$ M in the 1110−980 cm^{-1} spectral region. SEHRS: (A) −0.7, (B) −0.5, and (C) −0.3 V. SERS: (D) −0.7, (E) −0.5, and (F) −0.3 V. Same acquisition parameters as in Figure 16.

SEHRS band shifts 6 cm^{-1}, and the 1607 cm^{-1} SERS band shifts 5 cm^{-1}. Although increasing the potential to −0.05 V was required to produce a major spectral change (i.e., a new peak at 1635 cm^{-1}), the SEHRS spectra were so weak that the 1670−1545 cm^{-1} region was the only spectral region with an adequate signal-to-noise ratio. Consequently, Figures 18−20 show the potential-dependent behavior of both the SEHR and SER spectra of BPY at −0.7, −0.5, and −0.3 V only. Figure 18 shows essentially no potential-induced changes for either type of spectroscopy. In Figure 19, the 1016 cm^{-1} SEHRS band shifts 4 cm^{-1} whereas the 1014 cm^{-1} SERS band only shifts 1 cm^{-1}. Also, a SEHRS band at 1076 cm^{-1} grows in at −0.3 V. Figure 20 shows no changes in the SEHR spectra, yet a 2 cm^{-1} shift of the 769 cm^{-1} SERS band occurs. A complete listing of all of the vibrational

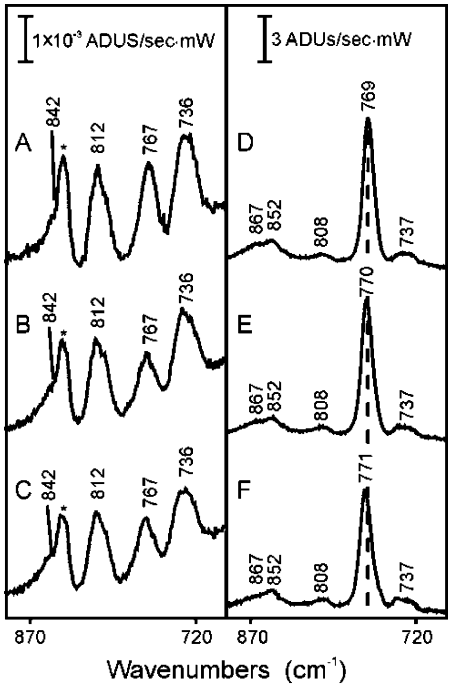

Figure 20. Potential dependence of the SEHR and SER spectra of BPY on a AgFON electrode with $[Cl^-] = 0.1$ M in the 880−710 cm^{-1} spectral region. SEHRS: (A) −0.7, (B) −0.5, and (C) −0.3 V. SERS: (D) −0.7, (E) −0.5, and (F) −0.3 V. Same acquisition parameters as in Figure 16.

Table 2. SEHRS and SERS Vibrational Frequencies at Various Applied Potentials vs Ag/AgCl for BPY at $\lambda_{ex} = 1064$ and 532 nm, Respectively[a]

	SEHRS				SERS		
trend	−0.3 V	−0.5 V	−0.7 V	trend	−0.3 V	−0.5 V	−0.7 V
					1635	1635	1635
S, W	1607	1605	1603	S	1612	1609	1607
				S	1515	1514	1513
	1486	1486	1486				
					1341	1341	1341
	1292	1292	1292		1295	1295	1295
	1233	1233	1233		1237	1237	1237
					1097	1097	1097
G	1076	1076			1077	1077	1077
	1065	1065	1065				
	1043	1043	1043				
S	1020	1018	1016		1015	1015	1014
					867	867	867
	842	842	842		852	852	852
	812	812	812		808	808	808
	767	767	767	S	771	770	769
	736	736	736		737	737	737
					673	673	673
					657	657	657
	626	626	626		625	625	625
					588	588	588
	571	571	571		570	570	570
					532	532	532
					519	519	519
					385	384	383
					353	353	353

[a] S = peak position shift; W = change in fwhm of peak; L = loss of peak

frequencies for BPY at −0.7, −0.5, and −0.3 V and their respective frequency shifts and spectral changes are listed in Table 2.

The changes observed in the BPY SEHR spectra are significantly less pronounced than those seen for the BPE data,

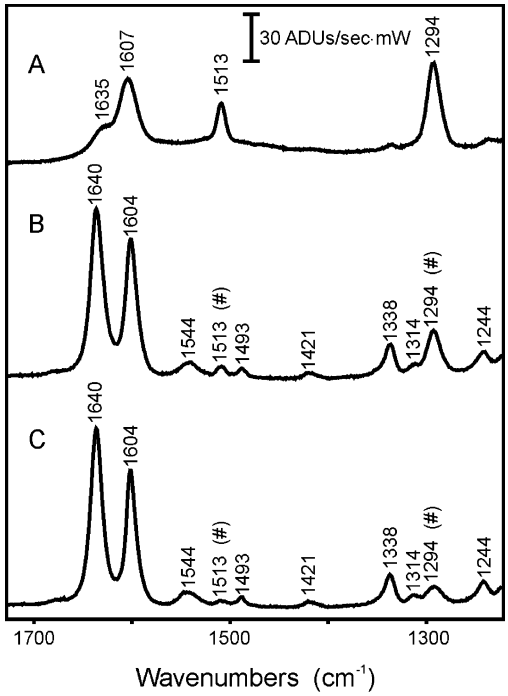

Figure 21. BPY/BPE adsorbate exchange probed by SERS on a AgFON electrode with $[Cl^-] = 0.1$ M, a fixed potential $E = -0.7$ V, 10 mW of $\lambda_{ex} = 532$ nm, and 60 s integration. (A) BPY as the initial adsorbate. (B) A solution containing BPE is allowed to flow into the cell. (C) A solution containing BPY is reintroduced into the cell. The (#) indicates residual BPY modes superimposed on the BPE SER spectrum.

and a much more positive potential, $E = -0.05$ V, was required to produce the new SEHRS band at 1635 cm^{-1}. To determine if this was a result of different adsorbate−surface binding strengths, we investigated the relative ΔG_{ads} between BPE and BPY on AgFON electrodes. Figure 21 shows the SER spectra resulting from an adsorbate exchange experiment at a fixed potential, $E = -0.7$ V. In this study, BPY was introduced into the electrochemical cell (Figure 21A), a solution containing BPE was allowed to flow into the cell (Figure 21B), and then a solution containing BPY was reintroduced into the cell (Figure 21C). It was found that BPE can displace BPY from the electrode surface, and upon reintroduction, BPY was unable to displace the adsorbed BPE. The residual BPY bands marked with a (#) in Figure 21 became weaker and weaker with time. Thus, BPE has a lower ΔG_{ads} than BPY (i.e., BPE binds more strongly). This result suggests that the strong versus weak adsorbate binding strength model (Figure 12C) is a viable co-contributing mechanism for the potential-dependent SEHR spectra. Because BPY binds less strongly to the Ag surface than BPE, BPY requires a more positive potential than BPE to produce the stronger binding characteristics that result in the altered SEHR spectra.

Conclusions

The first question addressed in this article was whether site symmetry reduction or the field gradient mechanism was the dominant process involved in dictating surface-enhanced vibrational spectra. If the symmetry of the centrosymmetric adsorbed species were lowered, then both the SEHR and SER spectra should have peaks of equal number and frequency, which was definitely not observed in our experiments. If the quadrupole field effect were active to the extent that has been previously described, then all major peaks in the SEHR spectra would be expected to exist in the SER spectra, which was also not the case.

Although not rigorously geometrically correct, this spectroscopic evidence suggests that the inversion symmetry of these molecules can be significantly retained upon surface adsorption on AgFON electrodes, and very few modes showed any evidence of symmetry lowering.

The second issue raised was whether SEHR spectra can give new molecular information compared to SERS. Upon potential excursions, the SEHR spectra were shown to change significantly, yet the SERS appeared to be insensitive to these changes in potential. We have concluded that the observed potential-induced changes in the SEHR spectra were a result of a combination of two effects: changes in the adsorption binding strength (ΔG_{ads}) and the presence of coadsorbed counterions. It appears that SEHRS is much more sensitive to local surface environmental changes than SERS. Therefore, there is definitely new chemical information contained in SEHRS studies that cannot be obtained through SERS.

Acknowledgment. We thank Professor George C. Schatz and Dr. Adam D. McFarland for stimulating discussion and helpful comments. This work was supported by the National Science Foundation, grants DMR-0076097/008, DMR-0520513, CHE-0414554, and by the AFOSR, grant F49620-02-1-0381.

LA0612264